

Signals of a 2 TeV W' boson and a heavier Z' boson

Bogdan A. Dobrescu and Patrick J. Fox

Theoretical Physics Department, Fermilab, Batavia, IL 60510, USA

November 5, 2015; revised April 8, 2016

Abstract

We construct an $SU(2)_L \times SU(2)_R \times U(1)_{B-L}$ model with a Higgs sector that consists of a bidoublet and a doublet, and with a right-handed neutrino sector that includes one Dirac fermion and one Majorana fermion. This model explains the Run 1 CMS and ATLAS excess events in the e^+e^-jj , jj , Wh^0 and WZ channels in terms of a W' boson of mass near 1.9 TeV and of coupling g_R in the 0.4–0.5 range, with the lower half preferred by limits on $t\bar{b}$ resonances and Run 2 results. The production cross section of this W' boson at the 13 TeV LHC is in the 700–900 fb range, allowing sensitivity in more than 17 final states. We determine that the Z' boson has a mass in the 3.4–4.5 TeV range and several decay channels that can be probed in Run 2 of the LHC, including cascade decays via heavy Higgs bosons.

Contents

1	Introduction	2
2	W' width and production cross section	3
3	$W' \rightarrow eN_D$ and N_D decay widths	8
4	Bosonic W' decays	12
5	Properties of the Z' boson	15
	5.1 Z' branching fractions	17
	5.2 Z' signals at the LHC	19
6	Conclusions	21

1 Introduction

The field content of the Standard Model (SM) of particle physics includes fermions, gauge bosons and a Higgs field. Quantum field theories whose low-energy limit is given by the SM often include a larger gauge group, an extended Higgs sector and additional fermions. Various theoretical constraints link the properties of these new fields, especially in connection to gauge symmetries and their spontaneous breaking. For example, the discovery of a W' boson (spin-1 field of electric charge ± 1) would imply the existence of a Z' boson (electrically-neutral spin-1 field), additional Higgs particles, and in many cases additional fermions.

Several excess events reported by the CMS [1, 2, 3, 4] and ATLAS [5] Collaborations based on the LHC Run 1 data hint towards a W' boson of mass in the 1.8–2 TeV range. An explanation for all these excess events is presented in [6] based on the $SU(2)_L \times SU(2)_R \times U(1)_{B-L}$ gauge group [7], with a Higgs sector consisting of a bidoublet scalar and an $SU(2)_R$ -triplet scalar. The phenomenological implications of that Higgs sector are discussed in [8], where it is shown that the W' decays into heavy Higgs bosons provide an explanation for a peculiar excess reported by ATLAS in final states with two leptons of the same charge and two or more b jets [9].

The $SU(2)_L \times SU(2)_R \times U(1)_{B-L}$ symmetry implies the existence of “right-handed” neutrinos. These usually have Majorana masses, or else have Dirac masses equal to those of the SM neutrinos. The CMS excess in the e^+e^-jj final state, and the absence of an e^+e^+jj excess imply that at least one of the right-handed neutrinos has a mostly Dirac mass at the TeV scale. As the right-handed neutrinos are two-component fermions, the question is which fermion fields do they partner with to become Dirac fermions? In [6, 8, 10] it is proposed that some new fermions become the Dirac partners of the right-handed neutrinos. A more intriguing possibility is that the electron and tau right-handed neutrinos form together a Dirac fermion as a result of a lepton-flavor symmetry [11]; this is related to the observation [12] that there is a special point in the parameter space of right-handed neutrino Majorana masses where the e^+e^+jj signal is suppressed.

Here we present a simpler $SU(2)_L \times SU(2)_R \times U(1)_{B-L}$ model that explains the CMS and ATLAS excess events. The Higgs sector includes only a bidoublet and an $SU(2)_R$ -doublet, which allows the Z' boson to have a mass as low as the current limit, of roughly 3 TeV. The right-handed neutrino sector includes a global symmetry forcing the electron and tau right-handed neutrinos to form a Dirac fermion. We analyze the LHC signatures

of this model, using Monte-Carlo simulations, and extract the region of parameter space consistent with the observed deviations from the SM. We find that simulations of different W' decay channels are required for this extraction due to contamination among signals.

In Section 2 we describe the model, we extract the value of the W' coupling consistent with the CMS dijet excess [2], and we compute the W' width and production cross section. In Section 3 we discuss the right-handed neutrino sector, and we show that the CMS e^+e^-jj excess is accommodated for a range of right-handed neutrino masses. W' decays into pairs of bosons are analyzed in Section 4. The properties of the Z' boson are studied in Section 5. Our conclusions are summarized in Section 6.

2 W' width and production cross section

We consider an $SU(3)_c \times SU(2)_L \times SU(2)_R \times U(1)_{B-L}$ gauge theory with the field content shown in Table 1. The right-handed neutrinos N_R^i (i labels the three generations) acquire masses at the TeV scale through the mechanism of Ref. [11], also discussed in section 3. The Higgs sector includes an $SU(2)_R$ doublet H_R whose VEV, of several TeV, breaks $SU(2)_R \times U(1)_{B-L}$ down to the SM hypercharge group $U(1)_Y$, and a bidoublet Σ whose VEV breaks $SU(2)_L \times U(1)_Y$ at the weak scale.

The only gauge fields beyond the SM are a W' boson and a Z' boson, which acquire masses primarily due to the H_R VEV. For $M_{W'} \approx 1.9$ TeV, as indicated by the 8 TeV LHC data, the Z' boson has a mass of a few TeV (discussed in Section 5). The VEV of the

Fields	spin	$SU(3)_c$	$SU(2)_L$	$SU(2)_R$	$U(1)_{B-L}$
$q_L^i = (u_L^i, d_L^i)^\top$	1/2	3	2	1	+1/3
$q_R^i = (u_R^i, d_R^i)^\top$	1/2	3	1	2	+1/3
$L_L^i = (\nu_L^i, \ell_L^i)^\top$	1/2	1	2	1	-1
$L_R^i = (N_R^i, \ell_R^i)^\top$	1/2	1	1	2	-1
Σ	0	1	2	2	0
H_R	0	1	1	2	1

Table 1: Fields carrying $SU(3)_c \times SU(2)_L \times SU(2)_R \times U(1)_{B-L}$ gauge charges. The index $i = 1, 2, 3$ labels the three generations of fermions.

bidoublet Σ leads to mass mixing between the $SU(2)_L \times SU(2)_R$ gauge bosons. The W boson and the hypothetical W' boson are linear combinations of the electrically-charged $SU(2)_L \times SU(2)_R$ gauge bosons, $W_L^{\pm\mu}$ and $W_R^{\pm\mu}$,

$$\begin{pmatrix} W_\mu^+ \\ W_\mu'^+ \end{pmatrix} = \begin{pmatrix} \cos \theta_+ & \sin \theta_+ \\ -\sin \theta_+ & \cos \theta_+ \end{pmatrix} \begin{pmatrix} W_{L\mu}^+ \\ W_{R\mu}^+ \end{pmatrix}, \quad (2.1)$$

with the $W_L - W_R$ mixing angle θ_+ given by [8]

$$\theta_+ = \frac{g_R}{g} \left(\frac{M_W}{M_{W'}} \right)^2 \sin 2\beta \left(1 + O(M_W^2/M_{W'}^2) \right). \quad (2.2)$$

The parameters introduced here are as follows: g_R is the $SU(2)_R$ gauge coupling, $g \approx 0.63$ is the SM weak coupling at 2 TeV, and the angle β arises from the usual $\tan \beta$ ratio of VEVs in the Two-Higgs doublet model, which is the manifestation of the bidoublet scalar Σ below the $SU(2)_R$ breaking scale.

The couplings of the W' boson to pairs of SM fermions, neglecting the $W_L - W_R$ mixing, are given by

$$\frac{g_R}{\sqrt{2}} W'_\mu (\bar{u}_R \gamma^\mu d_R + \bar{c}_R \gamma^\mu s_R + \bar{t}_R \gamma^\mu b_R) + \text{H.c.} \quad (2.3)$$

The quark fields here are in the mass eigenstate basis. Flavor-dependent perturbations to the above interactions are allowed by the $SU(2)_R$ gauge symmetry, but are constrained by measurements of flavor processes such as $K - \bar{K}$ meson mixing, and we assume here that they are negligible.

The couplings of the W' boson to pairs of SM bosons are fixed by gauge invariance and take the form [8]:

$$\begin{aligned} \mathcal{L}_{W'WZ} &= \frac{ig_R}{c_W} \left(\frac{M_W}{M_{W'}} \right)^2 \sin 2\beta \left[W_\mu'^+ \left(W_\nu^- \partial^{[\nu} Z^{\mu]} + Z_\nu \partial^{[\mu} W^{-\nu]} \right) + Z_\nu W_\mu^- \partial^{[\nu} W'^{+\mu]} \right] + \text{H.c.}, \\ \mathcal{L}_{W'Wh} &= -g_R M_W \sin(2\beta - \delta) W_\mu'^+ W^{\mu-} h^0 + \text{H.c.}, \end{aligned} \quad (2.4)$$

where $c_W \equiv \cos \theta_W \approx 0.87$ (θ_W is the weak mixing angle at the $M_{W'}$ scale), and $[\mu, \nu]$ represents the commutation of Lorentz indices. The WZ and Wh signals (see Section 4) indicate $0.36 \lesssim \tan \beta \lesssim 2.8$. The agreement between the SM predictions and the measured properties of h^0 requires the mixing angle between the neutral CP-even Higgs bosons, α , to be near the alignment limit. The amount by which the mixing deviates from the alignment limit is $\delta = \beta - \alpha - \pi/2 \ll 1$.

The W' partial widths into SM particles induced by the couplings shown in Eqs. (2.3) and (2.4) are given by [8]

$$\Gamma(W' \rightarrow t\bar{b}) \simeq \Gamma(W' \rightarrow c\bar{s}) = \Gamma(W' \rightarrow u\bar{d}) = \frac{g_R^2}{16\pi} M_{W'} \left(1 + \frac{\alpha_s}{\pi}\right) ,$$

$$\Gamma(W' \rightarrow WZ) \simeq \Gamma(W' \rightarrow Wh^0) \simeq \frac{g_R^2}{192\pi} \sin^2 2\beta M_{W'} . \quad (2.5)$$

The phase-space suppression factors (ignored here) give corrections of order $m_t^2/M_{W'}^2 \approx 0.8\%$ or $(M_h + M_W)^2/M_{W'}^2 \approx 1.2\%$ for $M_{W'} = 1.9$ TeV. The next-to-leading order (NLO) QCD corrections (included here) are of order 3%, with $\alpha_s \approx 0.1$ being the QCD coupling constant at the $M_{W'}$ scale.

Besides the branching fractions into SM particles, the W' boson can decay into a right-handed neutrino and an electron or τ , and also into two heavy Higgs bosons or one heavy Higgs boson and one SM boson. The absence of $\mu\mu jj$ signals in Run 1 of the LHC [1, 13] implies that the second-generation right-handed neutrino is heavier than (or nearly degenerate to) the W' .

The increase of the total width due to decays involving right-handed neutrinos (see Section 3) is between 4% and 12% (depending on the masses of right-handed neutrinos); an additional increase of up to 6% is due to decays involving heavy Higgs scalars (discussed in Section 4). Including these contributions, and taking the range for $\tan \beta$ into account, the total W' width is

$$\Gamma_{W'} \approx (31 - 35) \text{ GeV} \left(\frac{g_R}{0.5}\right)^2 \left(\frac{M_{W'}}{1.9 \text{ TeV}}\right) . \quad (2.6)$$

The W' coupling g_R can be determined from the cross section required to produce the dijet resonance near $M_{W'}$. The CMS dijet excess [3] at a mass in the 1.8–1.9 TeV range indicates that the W' production cross section times the dijet branching fraction is in the 100–200 fb range (this is consistent with the ATLAS dijet result [14], which shows a smaller excess at 1.9 TeV)¹. This was assumed in Refs. [6, 17] to be the range for $\sigma_{8jj}(W') \equiv \sigma(pp \rightarrow W' \rightarrow jj)_{\sqrt{s}=8 \text{ TeV}}$, where j is a hadronic jet associated with quarks or antiquarks other than the top. We point out here that the large W' mass implies that the CMS dijet search is also sensitive to merged jets arising from the decays of boosted top quarks and boosted W , Z or h^0 bosons produced in W' decays.

¹The CMS [15] dijet search with 2.4 fb⁻¹ of Run 2 data has a small excess (less than 2 σ) in the 1.7–1.8 TeV range that may be consistent with the Run 1 excess. The ATLAS [16] result with 3.6 fb⁻¹ of Run 2 data has no excess in the 1.8–2 TeV range, and sets a 95% CL upper limit on the dijet production cross section of around 300 fb at $M_{W'} = 1.9$ TeV. Reinterpreting this limit in our model we find $g_R \lesssim 0.44$.

To see that, note that the CMS search [3] identifies a narrow jet of cone $\Delta R \leq 0.5$, and then includes all hadronic activity in a wider cone of $\Delta R \leq 1.1$. This procedure is designed to collect all the radiation associated with the jet so that the invariant mass distribution is properly calibrated. An additional consequence of this procedure is that it cannot separate W' decays into two light jets from those into heavy SM particles that decay hadronically.

Consider first the $W' \rightarrow t\bar{b}$ channel. The case where the top quark decays hadronically implies that there is a narrow b jet back-to-back to a merged jet formed of three jets. As the CMS search is not using b -tagging, and the merged jet is typically much narrower than $\Delta R = 1.1$, this topology will contribute to the dijet peak near $M_{W'}$.

The case of semileptonic top decays is more complicated. The lepton is almost collinear with the jet arising from the top decay so that it usually does not pass the isolation requirement. The missing transverse energy carried by the neutrino is typically large enough to move the invariant mass of the system formed by the \bar{b} jet and the lepton-plus- b jet to values significantly lower than $M_{W'}$. Thus, the fraction of $W' \rightarrow t\bar{b}$ decays that contribute to the dijet peak near $M_{W'}$ is expected to be roughly given by $B(W' \rightarrow jj) \approx 67.4\%$. This would imply that combining the $W' \rightarrow t\bar{b}$ and $W' \rightarrow jj$ processes increases the number of dijet events by $\sim 34\%$ compared to the $W' \rightarrow jj$ process.

To improve this estimate, we have implemented the interactions (2.3) and (2.4) in FeynRules [18], which automatically generated the MadGraph [19] model files available at [20]. Using the Delphes [21] detector simulation and the NN23LO1 parton distributions [22], we find that $W' \rightarrow t\bar{b}$ increases the number of dijet events that pass the selection cuts and have an invariant mass above 1.7 TeV by 37% compared to $W' \rightarrow jj$ by itself.

A similar discussion applies to $W' \rightarrow WZ$ or Wh^0 . Events in which both the W and Z decay hadronically contribute to the dijet peak. These represent $B(W \rightarrow jj)B(Z \rightarrow jj) \approx 47.1\%$ of all $W' \rightarrow WZ$ events. In the case of $W' \rightarrow Wh^0$, the purely hadronic decays lead to a W merged jet back-to-back to a Higgs merged jet. The fraction of $W' \rightarrow Wh^0$ events that contribute to the dijet peak near $M_{W'}$ is expected to be $B(W \rightarrow jj)B(h^0 \rightarrow jj, 4j) \approx 54.1\%$, where $B(h^0 \rightarrow jj, 4j) \approx 80.2\%$ is the total hadronic branching fraction of the SM Higgs boson for $M_h = 125$ GeV [23]. Note that decays involving taus include missing energy so that their contribution to the dijet peak near $M_{W'}$ is suppressed.

Our simulations show that the contributions from $W' \rightarrow WZ$ and Wh^0 to the dijet peak are larger than the above estimates. However, given the small branching fractions of these modes, the increase in the number of dijet events that pass the selection cuts and

have an invariant mass above 1.7 TeV is only 4%.

Finally, the W' decays to heavy Higgs bosons (if kinematically open) also contribute to the dijet signal. The main channels, $W' \rightarrow H^\pm A^0$ and $H^\pm H^0$, followed by $H^\pm \rightarrow t\bar{t}$ and $A^0/H^0 \rightarrow t\bar{t}$ give two merged jets: one containing $Wb\bar{b}$ and the other one containing $W^+W^-b\bar{b}$. When these three W bosons decay hadronically (a 31% combined branching fraction), the reconstructed mass of the two merged jets is again near $M_{W'}$.

Summing over all these modes, we find that the total branching fraction of decays contributing to the dijet peak near $M_{W'}$ is $B(W' \rightarrow \text{dijet}) \approx 81 - 89\%$, with the uncertainty arising mainly due to the right-handed neutrino masses. The total production cross section at $\sqrt{s} = 8$ TeV required to explain the dijet peak is

$$\sigma_8(W') \approx \frac{100 - 200 \text{ fb}}{B(W' \rightarrow \text{dijet})} \approx 112 - 246 \text{ fb} . \quad (2.7)$$

This observed range needs to be compared with the predicted cross section. For $M_{W'} = 1.9$ TeV, the leading-order W' production cross section at $\sqrt{s} = 8$ TeV, computed with MadGraph, is 155 fb $(g_R/0.5)^2$. Next-to-leading order QCD effects can be taken into account by multiplying the leading-order cross section by $K_8(W') \approx 1.15$ [24] (this is consistent with the result of an MCFM [25] computation, but somewhat smaller than the K -factor computed in [26]). Thus, the predicted cross section is

$$\sigma_8(W') \approx 178 \text{ fb} \left(\frac{g_R}{0.5} \right)^2 . \quad (2.8)$$

Comparing Eqs. (2.7) and (2.8) allows us to determine the range for the W' coupling:

$$0.40 \lesssim g_R \lesssim 0.59 . \quad (2.9)$$

Combining this with Eq. (2.6) implies a total width $\Gamma_{W'} = 20\text{--}48$ GeV. Note that combining Run 1 and Run 2 dijet results reduces the required production cross section, but there is a theoretical lower bound $g_R > g_Y \approx 0.363$ (see section 5).

Searches for tb resonances using LHC Run 1 data impose a stronger upper limit on g_R . The semileptonic top decay is used by CMS [27] to set a cross section limit $\sigma(pp \rightarrow W' \rightarrow tb) < 100$ fb at the 95% CL. The hadronic top decay leads to a stronger CMS limit [28]: $\sigma(pp \rightarrow W' \rightarrow tb) < 60$ fb at the 95% CL. The combination [28] of these two tb final states gives $\sigma(pp \rightarrow W' \rightarrow tb) \lesssim 40$ fb for $M_{W'} = 1.9$ TeV. This implies $g_R \lesssim 0.45$. The ATLAS searches using semileptonic [29] and hadronic [30] top decays impose weaker upper limits on $\sigma(pp \rightarrow W' \rightarrow tb)$, of 120 fb and 210 fb, respectively. The discrepancy

between the CMS and ATLAS tb sensitivities in the case of hadronic top decays is due in part to the b tagging efficiencies, which are not well understood in the case of the large jet p_T associated with a resonance near 2 TeV.

The W' production at the 13 TeV LHC is 6.3 times larger than in Run 1,

$$\sigma_{13}(W') \approx 1130 \text{ fb} \left(\frac{g_R}{0.5} \right)^2, \quad (2.10)$$

taking into account a K -factor of $K_{13}(W') \approx 1.2$ [31]. For $0.4 < g_R < 0.44$ the Run 2 production cross section lies between 720 and 875 fb. Consequently, the existence of the W' can be tested in the $W' \rightarrow jj$ and $W' \rightarrow tb$ channels with $O(10)$ fb in Run 2.

3 $W' \rightarrow eN_D$ and N_D decay widths

An important component of a complete $SU(2)_L \times SU(2)_R \times U(1)_{B-L}$ model is the sector responsible for the right-handed neutrino masses. In this Section we analyze a mechanism that allows the three right-handed neutrinos to acquire masses consistent with the CMS e^+e^-jj excess [1] and the lack of a signal in related LHC searches (especially in the same-sign $eejj$ final state [32]). This mechanism does not require any field of mass below the $SU(2)_R \times U(1)_{B-L}$ breaking scale ($u_H \sim 5\text{--}7$ TeV) beyond those listed in Table 1. This relies, though, on higher-dimensional operators whose origin requires additional fields (discussed at the end of this Section) that have masses below ~ 20 TeV.

Let us consider the following lepton-number-violating dimension-5 operators:

$$-\frac{C_{e\tau}}{m_\psi^{e\tau}} (\bar{L}_R^e)^c H_R \tilde{H}_R L_R^\tau - \frac{C_{\mu\mu}}{2m_\psi^{\mu\mu}} (\bar{L}_R^\mu)^c H_R \tilde{H}_R L_R^\mu + \text{H.c.}, \quad (3.1)$$

where $\tilde{H}_R \equiv i\sigma_2 H_R^*$. The flavor structure of these operators is a consequence of the flavor symmetry introduced in [11]: a global $U(1)$ symmetry with L_R^e, L_R^μ, L_R^τ carrying charge $-1, 0, +1$, respectively. All other fields shown in Table 1 have global $U(1)$ charge 0. Replacing the $SU(2)_R$ doublet H_R by its VEV in Eq. (3.1) leads to the following mass matrix for right-handed neutrinos:

$$-u_H^2 \left[\frac{C_{e\tau}}{m_\psi^{e\tau}} \left((\bar{N}_R^e)^c N_R^\tau + (\bar{N}_R^\tau)^c N_R^e \right) + \frac{C_{\mu\mu}}{m_\psi^{\mu\mu}} (\bar{N}_R^\mu)^c N_R^\mu \right]. \quad (3.2)$$

Although these are Majorana masses, the N_R^e and N_R^τ fields form a Dirac fermion [11], labelled here N_D . This has a mass $m_{N_D} = C_{e\tau} u_H^2 / m_\psi^{e\tau}$, and its left- and right-handed

components are given by $N_{DL} \equiv (\bar{N}_R^c)^c$ and $N_{DR} \equiv N_R^c$, respectively. The muon right-handed neutrino N_R^μ remains a Majorana fermion of mass $m_{N^\mu} = C_{\mu\mu} u_H^2 / m_\psi^{\mu\mu}$.

The couplings of the W' boson to the Dirac fermion N_D , or the muon right-handed neutrino N_R^μ , and the SM charged leptons in the mass eigenstate basis follow from the $SU(2)_R$ gauge symmetry:

$$\frac{g_R}{\sqrt{2}} W'_\nu \left[\bar{N}_{DR} \gamma^\nu e_R + (\bar{N}_{DL})^c \gamma^\nu \tau_R + \bar{N}_R^\mu \gamma^\nu \mu_R \right] + \text{H.c.} \quad , \quad (3.3)$$

where the W' coupling g_R is the same as in Eq. (2.3).

As no $\mu\mu jj$ signal has been observed yet, we will assume the following mass hierarchy: $m_{N_D} < M_{W'} \lesssim m_{N^\mu}$. As a result, the $W' \rightarrow \mu N^\mu$ decay is kinematically closed or strongly phase-space suppressed, and we will ignore the presence of N_R^μ in what follows. The W' partial widths into a SM lepton and an N_D Dirac fermion follow from Eq. (3.3):

$$\Gamma(W' \rightarrow e N_D) = \Gamma(W' \rightarrow \tau N_D) = \frac{g_R^2}{48\pi} M_{W'} \left(1 + \frac{m_{N_D}^2}{2M_{W'}^2} \right) \left(1 - \frac{m_{N_D}^2}{M_{W'}^2} \right)^2 \quad . \quad (3.4)$$

The W' couplings shown in Eq. (3.3) also induce 3-body decays of the Dirac fermion N_D , through an off-shell W' . These have equal widths into $e^- u \bar{d}$ and $e^- c \bar{s}$ given by²

$$\Gamma(N_D \rightarrow e^- W'^* \rightarrow e^- u \bar{d}) = \frac{g_R^4 m_{N_D}^5}{2048\pi^3 M_{W'}^4} \left(1 + \frac{3m_{N_D}^2}{5M_{W'}^2} + \frac{2m_{N_D}^4}{5M_{W'}^4} + O(m_{N_D}^6/M_{W'}^6) \right) \quad . \quad (3.5)$$

For m_{N_D} close to $M_{W'}$ one has to use the exact formula for this width given in the Appendix. The width for $N_D \rightarrow e^- t \bar{b}$ is smaller:

$$\Gamma(N_D \rightarrow e^- W'^* \rightarrow e^- t \bar{b}) \simeq \Gamma(N_D \rightarrow e^- W'^* \rightarrow e^- u \bar{d}) f(m_{N_D}) \quad , \quad (3.6)$$

where the phase-space suppression is included in

$$f(m_{N_D}) = 1 - \frac{8m_t^2}{m_{N_D}^2} \left(1 - \frac{9m_{N_D}^2}{40M_{W'}^2} + O(m_{N_D}^4/M_{W'}^4) \right) + O\left((m_t/m_{N_D})^4 \ln(m_{N_D}/m_t) \right) \quad . \quad (3.7)$$

For m_{N_D} near m_t one needs to use Eq. (A.2). There is also a 2-body decay on N_D , proceeding through the small $W_L - W_R$ mixing:

$$\Gamma(N_D \rightarrow e^- W^+) = \frac{g_R^4 M_W^2 \sin^2 2\beta}{64\pi g^2 M_{W'}^4} m_{N_D}^3 \left(1 + 2 \frac{M_W^2}{m_{N_D}^2} \right) \left(1 - \frac{M_W^2}{m_{N_D}^2} \right)^2 \quad . \quad (3.8)$$

²Our result to leading order in m_{N_D} is larger by a factor of 2 than the corresponding one implied by Eq. (13) of [33], after taking into account the difference between Majorana and Dirac fermions (assuming that the ljj final state is defined there as the sum over $l = e, \mu, \tau$).

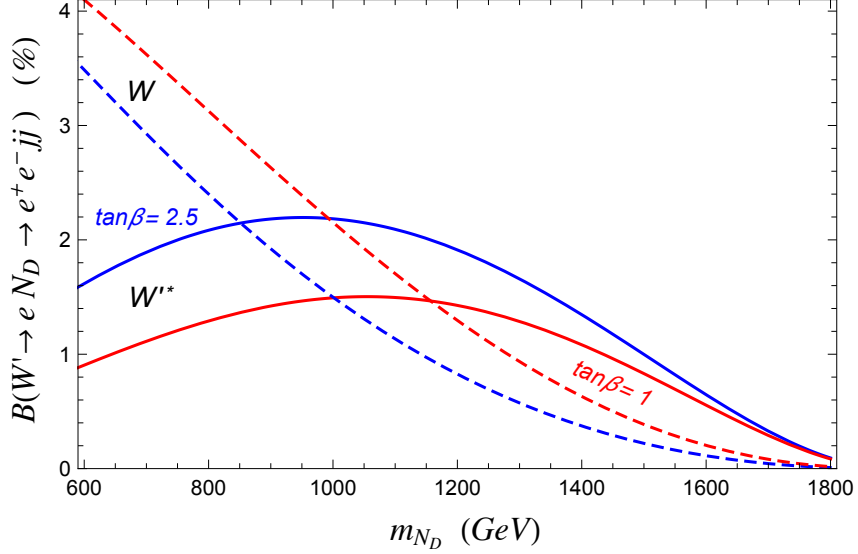


Figure 1: Branching fractions of the cascade decays $W' \rightarrow eN_D \rightarrow e^+e^-W'^* \rightarrow e^+e^-jj$ (solid lines) through an off-shell W' , and $W' \rightarrow eN_D \rightarrow e^+e^-W \rightarrow e^+e^-jj$ (dashed lines) through a SM W , where j is a jet arising from a quark (or antiquark) of the first or second generation. The parameters used here are $\tan\beta = 1$ or 2.5 , and $M_{W'} = 1.9$ TeV. The Dirac fermion N_D has couplings given in Eq. (3.3).

The W' couplings shown in Eq. (3.3) imply that the decays of N_D involving τ 's have opposite charges compared to the decays involving electrons [11]. The $N_D \rightarrow \tau^+W'^* \rightarrow \tau^+\bar{u}d$ or $\tau^+\bar{c}s$ widths are equal to that given in Eq. (3.5). Similarly, the $N_D \rightarrow \tau^+W'^* \rightarrow \tau^+\bar{t}b$ and $N_D \rightarrow \tau^+W^-$ decays have the same widths as those shown in Eqs. (3.6) and (3.8), respectively.

The branching fraction of the N_D 3-body decay into ejj is

$$B(N_D \rightarrow e^-W'^* \rightarrow e^-jj) = \frac{1}{2} \left(1 + \frac{1}{2}f(m_{N_D}) + \frac{16\pi^2 M_W^2}{g^2 m_{N_D}^2} \sin^2 2\beta \right)^{-1}, \quad (3.9)$$

where we ignored terms of order $M_W^4/m_{N_D}^4$. Multiplying this branching fraction by $B(W' \rightarrow eN_D)$ we obtain the total branching fraction shown in Figure 1.

Let us compare the CMS e^+e^-jj signal [1] with the predicted rate for $pp \rightarrow W' \rightarrow eN_D \rightarrow e^+e^-jj$. The acceptance-times-efficiency of the CMS event selection, estimated through our simulation, for events with $eejj$ mass above 1.8 TeV arising from the 3-body decay $N_D \rightarrow ejj$ decreases from 32% to 26% when m_{N_D} grows from 0.5 TeV to 1.6 TeV. The analogous acceptance-times-efficiency ranges for $N_D \rightarrow e\bar{t}b$ and $N_D \rightarrow e^-W^+$ are 28%–21% and 8.4%–7.2%, respectively. Given that there are 10 excess events, and the luminosity is 19.7 fb^{-1} , we obtain a central value for the signal cross section of 0.84

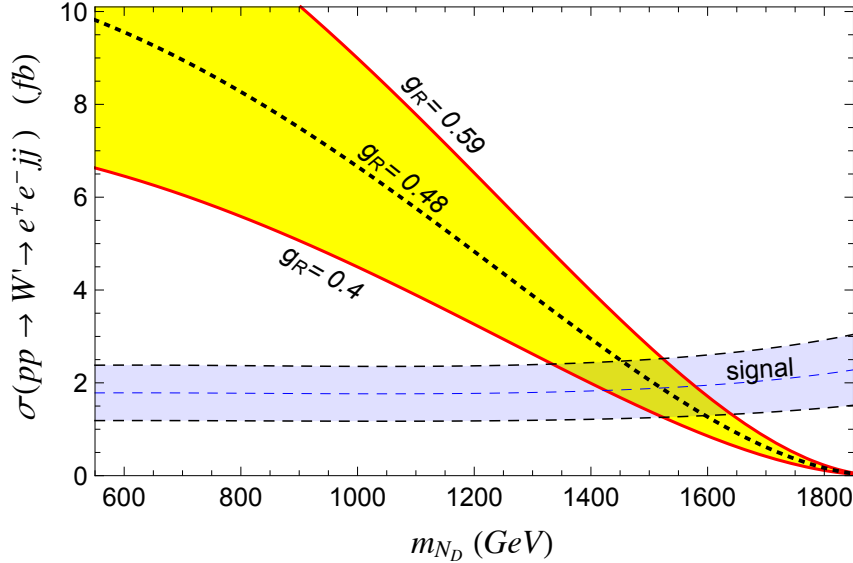


Figure 2: Cross section for $pp \rightarrow W' \rightarrow eN_D \rightarrow e^+e^-jj$ at $\sqrt{s} = 8$ TeV for $M_{W'} = 1.9$ TeV. The yellow shaded region between the two solid lines corresponds to the predicted cross section when g_R varies between 0.40 and 0.59. The dotted line represents the preferred value $g_R = 0.48$ (see Section 5.2). The band between dashed lines (labelled “signal”) represents the cross section required to explain the CMS e^+e^-jj signal (10 ± 3.3 events with $M_{eejj} > 1.8$ TeV).

fb. Including an uncertainty of ± 3.3 events gives the horizontal shaded band labelled “signal” in Figure 2. The predicted cross section for $pp \rightarrow W' \rightarrow eN_D \rightarrow e^+e^-jj$, given by $\sigma_8(W')B(W' \rightarrow eN_D \rightarrow e^+e^-jj)$, as a function of the N_D mass is within the shaded region between the two solid lines in Figure 2. That shaded region corresponds to $\sigma_8(W')$ in the 120–250 fb range (*i.e.*, $g_R = 0.4$ –0.59) and $\sin 2\beta = 1$, but it is almost insensitive to $\sin 2\beta$ in the 0.6–1 range (*i.e.*, $\tan \beta = 1$ –2.8). The large overlap of the predicted and observed signal regions is a significant success of our gauge-invariant W' model. The values of m_{N_D} that fit the $eejj$ signal are between 1.35–1.65 TeV, with some dependence on g_R .

The dimension-5 operators (3.1) arise from integrating out some fields. A simple choice is a set of three chiral fermions, $\psi_L^e, \psi_L^\mu, \psi_L^\tau$, which are $SU(3)_c \times SU(2)_L \times SU(2)_R \times U(1)_{B-L}$ singlets and carry global $U(1)$ charge $-1, 0, +1$, respectively. The most general mass terms invariant under the global $U(1)$ are $m_\psi^{e\tau}(\bar{\psi}_L^e)^c \psi_L^\tau + \text{H.c.}$ and $m_\psi^{\mu\mu}(\bar{\psi}_L^\mu)^c \psi_L^\mu$. These chiral fermions have Yukawa couplings to the $SU(2)_R$ -doublet leptons:

$$H_R (y_{e\psi} \bar{L}_R^e \psi_L^e + y_{e\psi} \bar{L}_R^\mu \psi_L^\mu + y_{\tau\psi} \bar{L}_R^\tau \psi_L^\tau) + \text{H.c.} \quad (3.10)$$

Integrating out the ψ_L fermions gives the operators (3.1), with coefficients $C_{e\tau} = y_{e\psi}y_{\tau\psi}$ and $C_{\mu\mu} = y_{\mu\psi}^2$.

4 Bosonic W' decays

In addition to the couplings to SM particles (see Section 2) and to right-handed neutrinos (see Section 3), the W' also has couplings to the heavy Higgs bosons present in the Σ bidoublet (H^\pm, H^0, A^0 , as in Two-Higgs-doublet models) and in the H_R doublet (a single neutral scalar, h_R^0). These couplings are due to the kinetic terms of the scalar fields and are determined by gauge invariance. For simplicity we assume that the Σ VEV is CP invariant, and that h_R^0 scalar is heavier than the W' boson.

The W' coupling to the W and a heavy neutral Higgs boson arises (up to negligible corrections of order $M_W^2/M_{W'}^2$) from the kinetic term of Σ :

$$g_R M_W W'_\mu{}^+ W^{-\mu} \left(\cos(2\beta - \delta) H^0 + i \cos 2\beta A^0 \right) + \text{H.c.} \quad (4.1)$$

By contrast, the kinetic terms of Σ and H_R have comparable contributions to the W' coupling to the Z and the heavy charged Higgs boson, with the sum given by

$$- g_R M_Z \cos 2\beta W'_\mu{}^+ Z^\mu H^- + \text{H.c.} \quad (4.2)$$

The W' couplings involving two charged Higgs bosons are, again, almost entirely due to the Σ kinetic term:

$$\frac{g_R}{2} W'_\mu{}^+ H^- \overleftarrow{\partial}^\mu \left(\sin 2\beta A^0 - i \sin(2\beta - \delta) H^0 - i \cos(2\beta - \delta) h^0 \right) + \text{H.c.} \quad (4.3)$$

The W' partial widths induced by the above couplings are

$$\begin{aligned} \Gamma(W' \rightarrow ZH^+) &\simeq \Gamma(W' \rightarrow WA^0) \simeq \frac{g_R^2 \cos^2 2\beta}{192\pi} M_{W'} \left(1 - \frac{M_{H^+}^2}{M_{W'}^2} \right)^3, \\ \Gamma(W' \rightarrow WH^0) &\simeq \Gamma(W' \rightarrow H^+h^0) \simeq \frac{g_R^2 \cos^2(2\beta - \delta)}{192\pi} M_{W'} \left(1 - \frac{M_{H^+}^2}{M_{W'}^2} \right)^3, \\ \Gamma(W' \rightarrow H^+A^0) &\simeq \Gamma(W' \rightarrow H^+H^0) \simeq \frac{g_R^2 \sin^2 2\beta}{192\pi} M_{W'} \left(1 - \frac{4M_{H^+}^2}{M_{W'}^2} \right)^{3/2}, \end{aligned} \quad (4.4)$$

where we have assumed that the heavy Higgs bosons have a common mass M_{H^+} and are sufficiently light so that corrections of order $M_h^2/(M_{W'} - M_{H^+})^2$ can be ignored. The

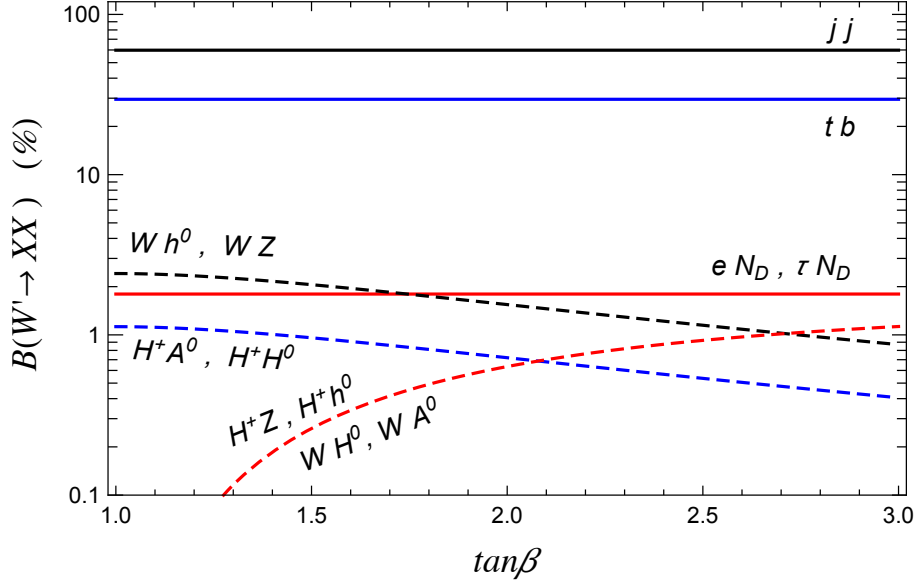


Figure 3: Branching fractions of the W' boson for $M_{W'} = 1.9$ TeV, $m_{N_D} = 1.5$ TeV, and common mass of 0.6 TeV for heavy Higgs bosons, in the alignment limit ($\delta = 0$). The lines labelled with two or more decay modes give the individual branching fractions.

corrections to each of these are given in [8]. As expected, the partial widths to modes related by Goldstone equivalence are equal, up to kinematic factors that have been ignored here. The W' branching fractions are displayed as a function of $\tan\beta$ in Figure 3.

The 3.4σ local excess in the ATLAS diboson resonance search with $WZ \rightarrow JJ$ [5] (J is a merged jet arising from a boosted W or Z) corresponds to 13 observed events of invariant mass $1.85 \text{ TeV} \leq m_{JJ} \leq 2.05 \text{ TeV}$, with an expected background of 5 events. In a related CMS analysis [34], which does not attempt to distinguish between W and Z merged jets, there is a smaller 1.3σ excess. If the ATLAS diboson excess is due to a W' decaying into WZ followed by hadronic decays of W and Z , then excess events should eventually also appear in other WZ decay channels at the same mass.

The branching fraction for $W' \rightarrow WZ \rightarrow \ell\ell\nu$ is too small to be useful in Run 1 (we expect less than 1 event to be observed in 20 fb^{-1} of 8 TeV data). The semileptonic channels, $WZ \rightarrow \ell\nu J$ and $WZ \rightarrow J\ell^+\ell^-$, however, are as sensitive to a W' as the $W' \rightarrow WZ \rightarrow JJ$ channel. The CMS search in the $WZ \rightarrow J\ell^+\ell^-$ channel has indeed yielded a 2σ excess at a mass in the 1.8–1.9 TeV range, while the CMS search in the $WZ \rightarrow \ell\nu J$ channel, which is slightly more sensitive, has only a 1σ excess in that mass range. The ATLAS searches in the semileptonic channels, however, are in good agreement with the background estimate. Given that the sensitivity in all these channels is

comparable, the ATLAS $WZ \rightarrow JJ$ result is in conflict at more than 2σ with the ATLAS combination of WZ semileptonic and leptonic channels [35]. This discrepancy may be due to a statistical fluctuation. We point out, however, that the resolution of this issue may be more convoluted. It may not be possible to analyze the WZ channels separately from other W' decay modes.

Consider first the $W' \rightarrow jj$ channel. The hadronic jets produced by a light quark have invariant masses that may be much larger than mass of the initial quark. Some of these jets may resemble a boosted W or Z decaying hadronically. Through simulation, we estimate that approximately 1% of the jj events give two jets with jet masses close to the W or Z mass. Even if $\sim 40\%$ of these jets fail jet grooming requirements [5], the branching fraction for $W' \rightarrow jj$ is ~ 30 larger than for $W' \rightarrow WZ$ and so this mode contributes a significant number of events to the JJ signal. A precise simulation of the event selection and detector effects in this channel is beyond the scope this work, but can be performed by the ATLAS and CMS collaborations.

Similarly, contributions to what appear to be $W' \rightarrow WZ \rightarrow JJ$ events may be due to other W' signals, including $W' \rightarrow tb$, $W' \rightarrow Wh^0$, $W' \rightarrow H^+A^0/H^0 \rightarrow (tb)(t\bar{t})$, etc. It is tempting to speculate that the whole ATLAS diboson excess is due to these other signals, in which case there would be no lower limit on the $W' \rightarrow WZ$ branching fraction (or equivalently on $\sin^2 2\beta$). However, the CMS $WZ \rightarrow J\ell^+\ell^-$ excess seems to contradict this possibility. Furthermore, the CMS search [2] for a Wh^0 resonance, with $W \rightarrow \ell\nu$ and $h^0 \rightarrow b\bar{b}$ has a 2.2σ excess, corresponding to 3 events with Wh^0 invariant mass between 1.8 TeV–1.9 TeV and 0.3 background events. In the alignment limit, the WZ and Wh^0 branching fractions are equal, so these observations place a lower limit on $\sin^2 2\beta$. The $pp \rightarrow W' \rightarrow WZ$ cross section that would account for the $WZ \rightarrow J\ell^+\ell^-$ and $Wh^0 \rightarrow \ell\nu b\bar{b}$ events is roughly in the 5–10 fb range, assuming the selection acceptance-times-efficiency for Wh^0 to be similar to that of $WZ \rightarrow JJ$, $0.1 \leq A \times \epsilon \leq 0.2$ [5]. This cross section indicates that these modes may have undergone a slight upward fluctuation and that $\sin 2\beta$ must be close to maximal. Assuming that the entire JJ excess does come from the WZ final state places a similar constraint, $0.5 \lesssim \tan \beta \lesssim 2.0$ for $g_R = 0.4$, and $0.36 \lesssim \tan \beta \lesssim 2.8$ for $g_R = 0.5$.

Recently, at Run 2 of the LHC, there have been searches for diboson final states. CMS, using 2.6 fb^{-1} of data, have searched for a resonance in both the $\ell\nu q\bar{q}$ and JJ final states [36], while ATLAS, using 3.2 fb^{-1} of data, have searched in the JJ final state [37]. Neither experiment has more than a 1σ excess in the region of $M_{W'} \approx 1.9 \text{ TeV}$. The

CMS result places the strongest constraint: $g_R \lesssim 0.46$ at $M_{W'} = 1.9$ TeV. This bound is comparable to that coming from the Run 2 ATLAS dijet resonance search [16], which is sensitive to the $W' \rightarrow jj$ channel. The Wh resonance search at Run 2 [38] has a small ($\sim 1.5\sigma$) excess at $M_{W'} = 1.9$ TeV, consistent with the Wh excess at the same mass in Run 1 [2].

Another interesting diboson channel is $W' \rightarrow WZ$ followed by $Z \rightarrow \nu\bar{\nu}$ and $W \rightarrow jj$ [39]. As the W and Z bosons are highly boosted, the first channel would appear as missing transverse energy (\cancel{E}_T) and a merged jet (J) of mass near M_W whose p_T is back-to-back with the \cancel{E}_T . The invariant mass distribution of the $J + \cancel{E}_T$ system (“merged mono-jet”) has a plateau-like shape that extends between a few hundred GeV and $M_{W'}$. The mono-jet searches [40, 41, 42] have produced an excess of events that may have a shape of this type, but it is too early to draw a conclusion as to whether its origin is new physics. With an increase in data, this will be an interesting search channel both in merged mono-jet and using sub-structure techniques.

There are additional diboson channels that, with more accumulated luminosity, will provide nontrivial tests of the W' properties. These involve some of the smaller W , Z , or h^0 branching fractions. Final states involving three or more leptons receive contributions from multiple topologies, each with different kinematics, *e.g.*, $W' \rightarrow WZ \rightarrow \ell\nu\ell\ell$ and $W' \rightarrow Wh^0 \rightarrow \ell\nu\ell\nu\ell\nu$. Both WZ and Wh^0 give contributions to final states with three taus.

Besides decays to SM bosons, W' bosons can generically decay into the heavy scalars associated with the Higgs sector responsible for breaking the extended gauge symmetry [43]. In the model discussed here, the W' decays into heavy Higgs bosons leads to top-rich final states, *e.g.*, $W' \rightarrow H^+A^0 \rightarrow t\bar{b}t\bar{t}$. As was pointed out in [8] these final states have the potential to explain the ATLAS same-sign leptons plus b -jets excess [9]. Due to differences in the structure of the right-handed neutrino sectors discussed here and in [8], the relative contributions from heavy Higgs and heavy neutrinos to the same-sign leptons plus b -jets final state is slightly altered.

5 Properties of the Z' boson

In addition to the electrically-charged gauge bosons, W_L^\pm and W_R^\pm (whose linear combinations give the W and W' bosons), the $SU(2)_L \times SU(2)_R \times U(1)_{B-L}$ gauge fields include

three electrically-neutral bosons: $W_L^{3\mu}$, $W_R^{3\mu}$, A_{B-L}^μ . Two linear combinations of these acquire masses due to the scalar VEVs, and become the Z and Z' bosons, while the third linear combination is the photon.

The VEVs of the bidoublet Σ and of the $SU(2)_R$ doublet H_R have the form

$$\langle \Sigma \rangle = v_H \begin{pmatrix} \cos\beta & 0 \\ 0 & e^{i\alpha_\Sigma} \sin\beta \end{pmatrix} \quad , \quad \langle H_R \rangle = \begin{pmatrix} 0 \\ u_H \end{pmatrix} \quad , \quad (5.1)$$

where $v_H \simeq \sqrt{2}M_W/g \approx 174$ GeV is the weak scale, and the $SU(2)_R \times U(1)_{B-L}$ breaking scale is

$$u_H \simeq \sqrt{2} \frac{M_{W'}}{g_R} \approx 5-7 \text{ TeV} \quad , \quad (5.2)$$

up to corrections of order $M_W^2/M_{W'}^2$. For simplicity, we assume that the CP-violating phase α_Σ vanishes. The VEVs in Eq. (5.1) induce mass terms for the electrically-neutral gauge bosons,

$$\frac{u_H^2}{4} (g_R W_R^{3\mu} - g_{B-L} A_{B-L}^\mu)^2 + \frac{v_H^2}{4} (g_L W_L^{3\mu} - g_R W_R^{3\mu})^2 \quad , \quad (5.3)$$

where $g_L \simeq g$ is the $SU(2)_L$ gauge coupling, and g_{B-L} is the $U(1)_{B-L}$ gauge coupling, which is related to the SM hypercharge gauge coupling ($g_Y \approx 0.363$ at 2 TeV) by

$$g_{B-L} = \left(\frac{1}{g_Y^2} - \frac{1}{g_R^2} \right)^{-1/2} \quad . \quad (5.4)$$

The mass terms in Eq. (5.3) lead to a 3×3 mass matrix of rank 2, which is diagonalized by the following unitary transformation that relates the photon (A^μ) and the Z and Z' bosons to the $SU(2)_L \times SU(2)_R \times U(1)_{B-L}$ gauge fields:

$$\begin{pmatrix} W_L^{3\mu} \\ W_R^{3\mu} \\ A_{B-L}^\mu \end{pmatrix} = \begin{pmatrix} s_W & c_W & -c_R \frac{g_R M_W^2}{g_L M_{Z'}^2} \\ s_R c_W & -s_R s_W & c_R \\ c_R c_W & -c_R s_W & -s_R \end{pmatrix} \begin{pmatrix} A^\mu \\ Z^\mu \\ Z'^\mu \end{pmatrix} \quad , \quad (5.5)$$

where we kept only the leading order in $M_W^2/M_{Z'}^2$, for each element of the matrix. In analogy to the SM $s_W \equiv \sin\theta_W$, we defined $s_R \equiv \sin\theta_R$ and $c_R \equiv \cos\theta_R$, with

$$c_R = \frac{g_R}{\sqrt{g_{B-L}^2 + g_R^2}} \quad , \quad (5.6)$$

which implies a simple relation between θ_R and g_R :

$$s_R = \frac{g_Y}{g_R} . \quad (5.7)$$

The mass of the Z' boson is related to the W' mass by

$$M_{Z'} = \frac{M_{W'}}{c_R} . \quad (5.8)$$

As the ranges for $M_{W'}$ and g_R can be derived from the W' signals, a range for $M_{Z'}$ can be predicted. We will show, however, that a more stringent lower limit on $M_{Z'}$ in this model is imposed by Z' searches in Run 1 of the LHC.

5.1 Z' branching fractions

The coupling of the Z' boson to a chiral fermion ψ is determined by the fermion's hypercharge (Y , in the normalization where the hypercharge of weak singlets equals their electric charge) and $SU(2)_R$ charge (T_R^3), and is given by

$$\frac{g_R}{c_R} (T_R^3 - Y s_R^2) Z'_\mu \bar{\psi} \gamma^\mu \psi . \quad (5.9)$$

As a result, the tree-level Z' decay widths into lepton pairs are

$$\begin{aligned} \Gamma(Z' \rightarrow e^+ e^-) &= \Gamma(Z' \rightarrow \mu^+ \mu^-) = \Gamma(Z' \rightarrow \tau^+ \tau^-) = \frac{g_R^2}{96\pi c_R^2} (1 - 4s_R^2 + 5s_R^4) M_{Z'} , \\ \Gamma(Z' \rightarrow N_D \bar{N}_D) &= \frac{g_R^2}{48\pi c_R^2} M_{Z'} \left(1 - \frac{4m_{N_D}^2}{M_{Z'}^2}\right)^{3/2} , \\ \Gamma(Z' \rightarrow \nu \bar{\nu}) &= \frac{g_R^2}{32\pi c_R^2} s_R^4 M_{Z'} . \end{aligned} \quad (5.10)$$

We assumed here that the $Z' \rightarrow N_R^\mu \bar{N}_R^\mu$ channel is kinematically closed. The Z' decay widths into quark-antiquark pairs are the same for the three fermion generations (the $m_t^2/M_{Z'}^2$ corrections are negligible), and given by

$$\begin{aligned} \Gamma(Z' \rightarrow u \bar{u}) &= \frac{g_R^2}{288\pi c_R^2} (9 - 24s_R^2 + 17s_R^4) M_{Z'} , \\ \Gamma(Z' \rightarrow d \bar{d}) &= \frac{g_R^2}{288\pi c_R^2} (9 - 12s_R^2 + 5s_R^4) M_{Z'} . \end{aligned} \quad (5.11)$$

The Z' also couples to pairs of gauge and Higgs bosons. The triple gauge boson couplings are fixed by gauge invariance, and the $Z'WW$ coupling is

$$ig_{RCR} \frac{M_W^2}{M_{Z'}^2} \left((W_\mu^- Z'_\nu - W_\nu^- Z'_\mu) \partial^\mu W^{+\nu} + \frac{1}{2} (W_\mu^+ W_\nu^- - W_\nu^+ W^{-\mu}) \partial^\mu Z'^\nu \right) + \text{H.c.} \quad (5.12)$$

The decay width is

$$\Gamma(Z' \rightarrow W^+ W^-) = \frac{g_R^2 c_R^2}{192\pi} M_{Z'} \quad . \quad (5.13)$$

If heavy enough, *i.e.* $c_R < 1/2$, the Z' can decay to a pair of W' bosons,

$$\Gamma(Z' \rightarrow W' W') = \frac{g_R^2}{192\pi c_R^2} \left(1 + 20 \frac{M_{W'}^2}{M_{Z'}^2} + 12 \frac{M_{W'}^4}{M_{Z'}^4} \right) \left(1 - 4 \frac{M_{W'}^2}{M_{Z'}^2} \right)^{3/2} M_{Z'} \quad . \quad (5.14)$$

The Z' has couplings to the five Higgs bosons coming from the Σ bidoublet (h^0, H^0, A^0, H^\pm) as well as the single scalar (h_R^0) left after the doublet H_R VEV breaks $SU(2)_R \times U(1)_{B-L}$ to $U(1)_Y$. We will assume that h_R^0 is too heavy to be involved in Z' decays. The relevant couplings controlling the decay of Z' to final states involving two Higgs bosons are

$$\frac{g_{RCR}}{2} Z'_\mu \left(\sin \delta h \overleftrightarrow{\partial}^\mu A^0 + \cos \delta H \overleftrightarrow{\partial}^\mu A^0 + i H^- \overleftrightarrow{\partial}^\mu H^+ \right) \quad . \quad (5.15)$$

If all the heavy Higgses are lighter than $M_{Z'}/2$ the decay widths that survive in the alignment limit are

$$\begin{aligned} \Gamma(Z' \rightarrow H^0 A^0) &\simeq \frac{g_R^2 c_R^2 \cos^2 \delta}{192\pi} M_{Z'} \left(1 - \frac{4M_{H^+}^2}{M_{Z'}^2} \right)^{3/2} \quad , \\ \Gamma(Z' \rightarrow H^+ H^-) &\simeq \frac{g_R^2 c_R^2}{192\pi} M_{Z'} \left(1 - \frac{4M_{H^+}^2}{M_{Z'}^2} \right)^{3/2} \quad . \end{aligned} \quad (5.16)$$

where we assumed as in Section 4 that $M_{A^0} \simeq M_{H^0} \simeq M_{H^+}$. The couplings of the Z' to one Higgs boson and one gauge boson are

$$g_{RCR} M_Z Z'_\mu Z^\mu (\cos \delta h^0 - \sin \delta H^0) \quad , \quad (5.17)$$

and the corresponding width is

$$\Gamma(Z' \rightarrow Z h^0) \simeq \frac{g_R^2 c_R^2 \cos^2 \delta}{192\pi} M_{Z'} \quad . \quad (5.18)$$

Note that the Z boson here, as well as the W bosons in Eq. (5.13), are longitudinally polarized [44], so as expected based on the equivalence theorem the widths for $Z' \rightarrow WW$ and $Z h^0$ are approximately equal in the alignment limit. Furthermore, since the

longitudinal W and Z are part of the same Higgs bidoublet field with the heavy Higgs bosons, the widths for $Z' \rightarrow H^0 A^0$ and $H^+ H^-$ shown in Eq. (5.16) are equal to those for $Z' \rightarrow Z h^0$ and WW in the limit where phase space suppression is negligible.

There are two further modes that are negligible in the alignment limit,

$$\Gamma(Z' \rightarrow ZH^0) \simeq \Gamma(Z' \rightarrow h^0 A^0) \simeq \frac{g_R^2 c_R^2 \sin^2 \delta}{192\pi} M_{Z'} \left(1 - \frac{M_{H^+}^2}{M_{Z'}^2}\right)^3. \quad (5.19)$$

The decays to $H^+ W^-$, $H^+ W'^-$ and WW' are suppressed by $M_Z^2/M_{Z'}^2$, and so are too small to be of interest at present. There are also 3-body decays that have small branching fractions and we ignore here.

Based on Eqs. (5.10)-(5.18), we find the Z' branching fractions shown in Figure 4. The parameters used there are $M_{W'} = 1.9$ TeV (other values of $M_{W'}$ in the 1.8–2 TeV range imply a different s_R , leading to slight changes in the Z' branching fractions), $m_{N_D} = 1.5$ TeV (the branching fractions other than $N_D \bar{N}_D$ are rather insensitive to m_{N_D}), and a common mass of 600 GeV for the heavy Higgs bosons from the bidoublet (only the $H^0 A^0$ and $H^+ H^-$ branching fractions are sensitive to this choice). Note that in the alignment limit the partial widths have no dependence on $\tan \beta$. One should keep in mind that if the assumptions $m_{N^\mu} > M_{Z'}/2$ and $M_{h_R} > M_{Z'}$ used here turn out to be false, the $Z' \rightarrow N_R^\mu \bar{N}_R^\mu$ and $Z' \rightarrow Z h_R^0$ channels may prove to be important.

5.2 Z' signals at the LHC

From Eq. (5.9) it follows that the dominant Z' production at hadron colliders is through its coupling to right-handed down quarks. The Z' couplings depend on g_R , which in turn depends on $M_{Z'}$ for fixed $M_{W'}$ [see Eq. (5.8)]. For $M_{W'} = 1.9$ TeV and g_R in the range shown in Eq. (2.9) we find $M_{Z'}$ in the 2.4–4.5 TeV range.³ As no dilepton events of invariant mass above 1.8 TeV has been observed in Run 1 of the LHC, the lower part of the $M_{Z'}$ mass range can be ruled out. To derive the lower limit on $M_{Z'}$, we require less than three predicted $Z' \rightarrow \ell^+ \ell^-$ events in the dilepton searches performed by ATLAS [46] and CMS [47] taken together. The Z' production cross section at the 8 TeV LHC, obtained by multiplying the MadGraph result with $K(Z') = 1.16$ [46], decreases from 1.6 fb for $M_{Z'} = 2.8$ TeV to 1.1 fb for $M_{Z'} = 2.9$ TeV. The acceptance-times-efficiency in the dielectron (dimuon) channel is 65% (40%) at ATLAS [46] and 55% (80%) at CMS [47].

³Similar $M_{Z'}$ ranges have been discussed in related models [45].

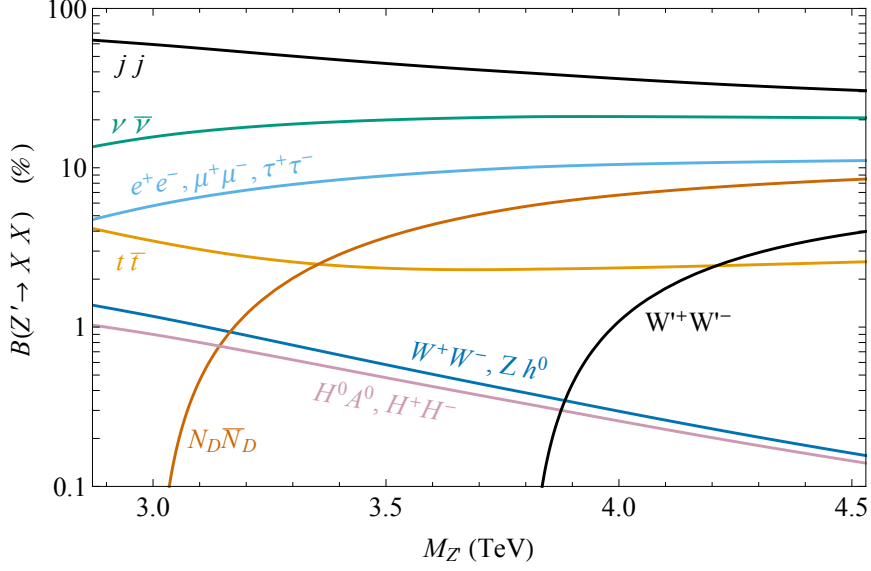


Figure 4: Branching fractions of the Z' boson for $M_{W'} = 1.9$ TeV, $m_{N_D} = 1.5$ TeV, and $M_{H^+} = M_{H^0} = M_{A^0} = 600$ GeV in the alignment limit ($\delta = 0$). The jj line is the sum of the partial widths for $u\bar{u}$, $d\bar{d}$, $s\bar{s}$, $c\bar{c}$, and $b\bar{b}$; the $\nu\bar{\nu}$ line is the sum of partial widths into SM neutrinos; the lines labelled with two or more decay modes give the individual branching fractions.

Using the $Z' \rightarrow \ell^+\ell^-$ branching fraction shown in Figure 4, we conclude that the lower limit on $M_{Z'}$ set by the Run 1 searches is approximately 2.85 TeV. Thus, the range of $M_{Z'}$ relevant for this model is $2.9 \text{ TeV} \lesssim M_{Z'} \lesssim 4.5 \text{ TeV}$.

The Z' production cross section at the 13 TeV LHC, computed at leading order with MadGraph and multiplied by $K(Z') = 1.16$ is shown in Figure 5. A Z' whose mass saturates the Run 1 bound has a production cross section of ~ 19 fb at Run 2, which predicts approximately five dilepton Z' events after 5 fb^{-1} . Although after 65 pb^{-1} CMS observed a dielectron event [48] with invariant mass of 2.9 TeV (the probability for this event to be due to the SM background is $\sim 10^{-3}$) the more recent Run 2 analyses of CMS [49] and ATLAS [50] have no deviation from the SM prediction. The ATLAS result, using 3.2 fb^{-1} , places a lower bound of 3.4 TeV on the Z' mass, corresponding to $g_R = 0.44$ and a total width of $\Gamma_{Z'} \approx 80$ GeV.

The dominant branching fraction is $Z' \rightarrow jj$ (see Figure 4). Furthermore, Higgs bosons lighter than ~ 1 TeV and SM bosons or top quarks, produced in the decay of the Z' , will be sufficiently boosted that their decay products will lie in a single jet. Thus, the effective dijet branching fraction for a 2.9 TeV Z' , and $g_R = 0.48$, increases from 62% to about 70%,

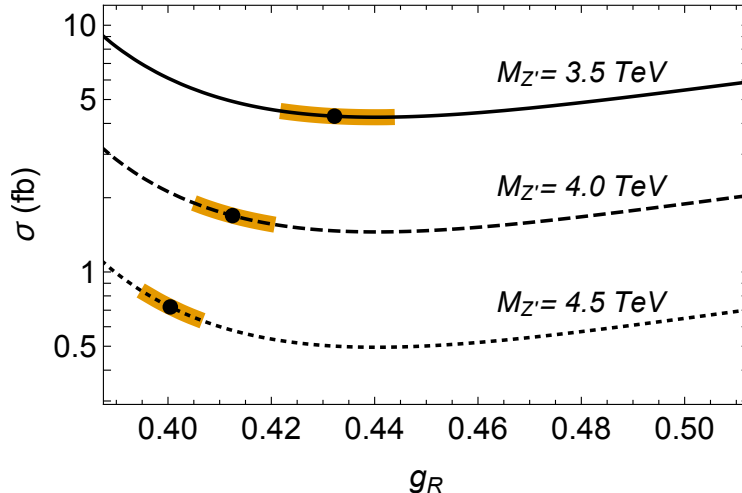


Figure 5: Production cross section, including a K -factor of 1.16, for a Z' boson of mass 3.5, 4, and 4.5 TeV at the LHC with $\sqrt{s} = 13$ TeV. The thicker region of each curve denotes the range of g_R for which $1.8 \leq M_{W'} \leq 2$ TeV, with the marked point at $M_{W'} = 1.9$ TeV.

with the remaining 30% due to 5% for each of e^+e^- , $\mu^+\mu^-$ and $\tau^+\tau^-$, and a 14% invisible branching fraction; we have assumed that N_D is heavier than $M_{Z'}/2$. Assuming the acceptance-times-efficiency for these high p_T jets coming from Z' decay is approximately 50% at both CMS and ATLAS we estimate that the signal in each experiment is ~ 8 dijet events with invariant mass around 3 TeV in Run 1. This signal is too small compared to the QCD background [3, 14].

After 30 fb^{-1} of Run 2 each experiment, assuming a similar acceptance and efficiency as in Run 1, should have ~ 200 dijet events. The sizable QCD background makes this a challenging search channel, although it may be possible to use various signal features, including angular distributions, quark-versus-gluon discriminants, and substructure techniques (for the hadronic decays of boosted objects) to reduce the background.

6 Conclusions

The CMS and ATLAS Collaborations, analyzing LHC Run 1 data, have accumulated an intriguing set of excess events over disparate final states. These include excesses near 2 TeV in jj , WZ , Wh and e^+e^-jj resonance searches [1]-[5], as well as an excess in the final state with same-sign leptons plus b jets [9]. We have shown that there is a common explanation for all these excess events in a model with $SU(3)_c \times SU(2)_L \times SU(2)_R \times$

$U(1)_{B-L}$ gauge structure, a Higgs sector with only a bidoublet and an $SU(2)_R$ doublet, and a flavor symmetry that controls the masses of the right-handed neutrinos. We refer to this as the $Re\tau D$ model, to emphasize that there is a flavor symmetry acting on the e and τ right-handed neutrinos, and that the $SU(2)_R \times U(1)_{B-L}$ symmetry is broken by a Doublet.

Let us briefly mention some differences between this model and the “RDiT model” presented in [6, 8] and the “ $Re\tau T$ model” presented in [11]. Both RDiT and $Re\tau T$ use an $SU(2)_R$ Triplet to break the $SU(2)_R \times U(1)_{B-L}$ gauge symmetry. As a result, the relation between the W' and Z' masses shown in Eq. (5.8) for our $Re\tau D$ model is modified by a factor of $\sqrt{2}$, pushing the Z' mass above 3.5 TeV. The RDiT model has Dirac masses for right-handed neutrinos, with the left-handed Dirac partners provided by vectorlike $SU(2)_R$ -doublet leptons. As a result, there is an additional parameter that controls the W' coupling to an electron and a Dirac right-handed neutrino. By contrast, in the $Re\tau T$ model and our $Re\tau D$ model the e and τ right-handed neutrinos form a Dirac fermion (N_D), whose mass must be in the 1.4–1.6 TeV range (see Figure 2) to explain the CMS e^+e^-jj excess.

The excess events from Run 1, taken together, point towards a W' of mass ~ 1.9 TeV, which means that the decay products of the W' are highly boosted. The jj excess is not only sensitive to W' decays to light quarks but also to its decays to heavy SM particles, which subsequently decay hadronically. This raises the *effective* hadronic branching fraction from $\sim 60\%$ to 80 – 90%. We take this effect into account and reanalyze the dijet excess and determine that the range necessary to explain the excess is $0.4 \lesssim g_R \lesssim 0.59$, corresponding to a W' width of 20 – 48 GeV. We also point out that the lack of an excess in the CMS tb resonance search places a nontrivial constraint, $g_R \lesssim 0.45$, while the constraints from ATLAS are considerably weaker and allow the whole coupling range favored by the dijet excess.

An upper limit on g_R is placed by dilepton resonance searches in Run 2: the $M_{Z'} \gtrsim 3.4$ TeV limit corresponds to $g_R \lesssim 0.44$ in this $Re\tau D$ model. A comparable limit on g_R is set by the Run 2 dijet searches. The only other relevant parameters are $\tan \beta$, which controls the $W' \rightarrow WZ$ and $W' \rightarrow Wh^0$ branching fractions, and the masses of the heavy Higgs bosons. The Run 1 diboson events indicate $0.35 \lesssim \tan \beta \lesssim 2.8$ (see Section 4), while the ATLAS events with same-sign leptons plus b jets prefer $M_{H^+} \simeq M_{H^0} \simeq M_{A^0} \approx 500\text{--}600$ GeV [8].

Our MadGraph model files [20] include all the new particles discussed here: W' , Z' ,

N_D, H^+, H^0, A^0 . These allow simulations of the many signals predicted in this model, and can be used by the experimental collaborations to disentangle the cross-contamination of new-physics channels (*e.g.*, $W' \rightarrow jj$ versus $W' \rightarrow WZ \rightarrow JJ$, mentioned in Section 4).

There are many W' decays that can be tested in Run 2. From Figure 3, it follows that there are at least 7 channels with branching fractions at percent level or above. The N_D fermion produced in two of these channels has several decay modes: ejj, etb, eW (as well as others with small branching fractions, including eWh and eWZ) and the same with e replaced by τ . We thus obtain more than 17 final states (without even counting the various decay modes of the SM bosons) in which the LHC Run 2 will have sensitivity to the existence of the W' boson.

The Z' presents a separate set of opportunities. Taking into account the W' mass and production cross section that fit the Run 1 dijet excess and the lower $M_{Z'}$ limit set by Run 2, the Z' mass is in the 3.4 – 4.5 TeV range. The Z' branching fractions, shown in Figure 4, are large enough to allow sensitivity in 9 channels, with many additional ones (originating from $N_D\bar{N}_D$ and $W'W'$) opening up for large enough $M_{Z'}$.

Acknowledgments: We would like to thank Dan Amidei, David Calvet, John Campbell, Richard Cavanaugh, Pilar Coloma, Frank Deppisch, Wade Fisher, Mike Hance, Philip Harris, Robert Harris, James Hirschauer, Zhen Liu, Jeremy Love, Sho Maruyama, Steve Mrenna, Natsumi Nagata, Jianming Qian, Martin Schmaltz, Jacob Searcy, Karishma Sekhon, Nhan Tran, Bing Zhou and Junjie Zhu, for helpful conversations and comments.

Appendix: Right-handed neutrino width

The 3-body decays of the right-handed neutrino (see Section 3) proceed through an off-shell W' . The squared matrix element for the $N_D \rightarrow et\bar{b}$ decay, summed over final states and averaged over the initial one is

$$\frac{3g_R^4}{2(m_{12}^2 - M_{W'}^2)^2} \left[m_{23}^2 \left(m_{N_D}^2 + m_t^2 - m_{23}^2 - \frac{m_{N_D}^2 m_t^2}{M_{W'}^2} \right) + \frac{m_{N_D}^2 m_t^2}{4M_{W'}^4} (m_{N_D}^2 - m_{12}^2) (m_{12}^2 - m_t^2) \right]. \quad (\text{A.1})$$

Here m_{12} and m_{13} are the invariant masses of the $t\bar{b}$ and $e\bar{b}$ systems, respectively. After integrating over phase space we find the following width:

$$\begin{aligned} \Gamma(N_D \rightarrow e^- t \bar{b}) &= \frac{3g_R^4 m_{N_D}^5}{(8\pi)^3 M_{W'}^4} \left[\frac{M_{W'}^6}{m_{N_D}^6} \left(1 - \frac{m_t^2}{m_{N_D}^2}\right) \left(1 - \frac{m_{N_D}^4 + m_t^4 - m_{N_D}^2 m_t^2/2}{6M_{W'}^4} + \frac{m_{N_D}^4 m_t^4}{4M_{W'}^8}\right) \right. \\ &+ \frac{M_{W'}^8}{m_{N_D}^8} \left(1 - \frac{m_{N_D}^2}{M_{W'}^2}\right) \left(1 - \frac{m_t^2}{M_{W'}^2}\right) \left(1 - \frac{m_{N_D}^2 m_t^2}{4M_{W'}^4} \left(1 + \frac{m_t^2}{M_{W'}^2}\right) \left(1 + \frac{m_{N_D}^2}{M_{W'}^2}\right)\right) \ln \frac{M_{W'}^2 - m_{N_D}^2}{M_{W'}^2 - m_t^2} \\ &\left. - \frac{M_{W'}^4}{2m_{N_D}^4} \left(1 - \frac{m_t^4}{m_{N_D}^4}\right) \left(1 + \frac{5m_{N_D}^2 m_t^2}{4M_{W'}^4}\right) + 2 \frac{m_t^4}{m_{N_D}^4} \left(1 + \frac{m_{N_D}^2 m_t^2}{4M_{W'}^4}\right) \ln \frac{m_{N_D}}{m_t} \right]. \quad (\text{A.2}) \end{aligned}$$

In the limit $m_t \rightarrow 0$ this is equal to the width for $N_D \rightarrow e^- u \bar{d}$:

$$\Gamma(N_D \rightarrow e^- u \bar{d}) = \frac{3g_R^4 M_{W'}^4}{(8\pi)^3 m_{N_D}^3} \left[\left(1 - \frac{m_{N_D}^2}{M_{W'}^2}\right) \ln \left(1 - \frac{m_{N_D}^2}{M_{W'}^2}\right) + \frac{m_{N_D}^2}{M_{W'}^2} - \frac{m_{N_D}^4}{2M_{W'}^4} - \frac{m_{N_D}^6}{6M_{W'}^6} \right]. \quad (\text{A.3})$$

Expanding this expression in $m_{N_D}^2/M_{W'}^2$ gives Eq. (3.5), while expanding Eq. (A.2) in both m_t/m_{N_D} and $m_{N_D}/M_{W'}$ gives Eq. (3.6).

References

- [1] V. Khachatryan *et al.* [CMS Collaboration], ‘‘Search for heavy neutrinos and W bosons with right-handed couplings in pp collisions at $\sqrt{s} = 8$ TeV,’’ *Eur. Phys. J. C* **74**, no. 11, 3149 (2014) [arXiv:1407.3683 [hep-ex]].
- [2] CMS Collaboration, ‘‘Search for massive WH resonances decaying to $\ell\nu b\bar{b}$ final state in the boosted regime at $\sqrt{s} = 8$ TeV,’’ note PAS-EXO-14-010, March 2015.
- [3] V. Khachatryan *et al.* [CMS Collaboration], ‘‘Search for resonances and quantum black holes using dijet mass spectra in pp collisions at $\sqrt{s} = 8$ TeV,’’ *Phys. Rev. D* **91**, no. 5, 052009 (2015) [arXiv:1501.04198].
- [4] V. Khachatryan *et al.* [CMS Collaboration], ‘‘Search for massive resonances decaying into pairs of boosted bosons in semi-leptonic final states at $\sqrt{s} = 8$ TeV,’’ *JHEP* **1408**, 174 (2014) [arXiv:1405.3447].
- [5] G. Aad *et al.* [ATLAS Collaboration], ‘‘Search for high-mass diboson resonances with boson-tagged jets in pp collisions at $\sqrt{s} = 8$ TeV,’’ arXiv:1506.00962 [hep-ex].

- [6] B. A. Dobrescu and Z. Liu, “A W' boson near 2 TeV: predictions for Run 2 of the LHC,” arXiv:1506.06736 [hep-ph].
- [7] R. E. Marshak and R. N. Mohapatra, “Quark-lepton symmetry and B-L as the $U(1)$ generator of the electroweak symmetry group,” Phys. Lett. B **91**, 222 (1980); “Local B-L symmetry of electroweak interactions, Majorana neutrinos and neutron oscillations,” Phys. Rev. Lett. **44**, 1316 (1980).
 Earlier proposals for an $SU(2)_L \times SU(2)_R \times U(1)$ gauge symmetry had the normalization of the quark $U(1)$ charges inconsistent with the modern understanding of hypercharges: J. C. Pati and A. Salam, “Lepton number as the fourth color,” Phys. Rev. D **10**, 275 (1974). R. N. Mohapatra and J. C. Pati, “Left-right gauge symmetry and an isoconjugate model of CP violation,” Phys. Rev. D **11**, 566 (1975); “A natural left-right symmetry,” Phys. Rev. D **11**, 2558 (1975). G. Senjanovic and R. N. Mohapatra, “Exact left-right symmetry and spontaneous violation of parity,” Phys. Rev. D **12**, 1502 (1975);
 For a review, see P. Duka, J. Gluza and M. Zralek, “Quantization and renormalization of the manifest left-right symmetric model of electroweak interactions,” Annals Phys. **280**, 336 (2000) [hep-ph/9910279].
- [8] B. A. Dobrescu and Z. Liu, “Heavy Higgs bosons and the 2 TeV W' boson,” arXiv:1507.01923 [hep-ph].
- [9] G. Aad *et al.* [ATLAS Collaboration], “Analysis of events with b -jets and a pair of leptons of the same charge in pp collisions at $\sqrt{s} = 8$ TeV,” JHEP **1510**, 150 (2015) [arXiv:1504.04605 [hep-ex]].
- [10] P. S. B. Dev and R. N. Mohapatra, “Unified explanation of the $eejj$, diboson and dijet resonances at the LHC,” arXiv:1508.02277 [hep-ph].
 F. F. Deppisch, L. Graf, S. Kulkarni, S. Patra, W. Rodejohann, N. Sahu and U. Sarkar, “Reconciling the 2 TeV excesses at the LHC in a Linear Seesaw Left-Right Model,” arXiv:1508.05940 [hep-ph].
 See also J. A. Aguilar-Saavedra and F. R. Joaquim, “Closer look at the possible CMS signal of a new gauge boson,” Phys. Rev. D **90**, no. 11, 115010 (2014) [arXiv:1408.2456]; F. F. Deppisch, T. E. Gonzalo, S. Patra, N. Sahu and U. Sarkar, “Signal of right-handed charged gauge bosons at the LHC?,” Phys. Rev. D **90**, no. 5, 053014 (2014) [arXiv:1407.5384 [hep-ph]].

- [11] P. Coloma, B. A. Dobrescu and J. Lopez-Pavon, “Right-Handed Neutrinos and the 2 TeV W' Boson,” arXiv:1508.04129 [hep-ph].
- [12] J. Gluza and T. Jelinski, “Heavy neutrinos and the $pp \rightarrow lljj$ CMS data,” Phys. Lett. B **748**, 125 (2015) [arXiv:1504.05568 [hep-ph]].
- [13] G. Aad *et al.* [ATLAS Collaboration], “Search for heavy Majorana neutrinos with the ATLAS detector in pp collisions at $\sqrt{s} = 8$ TeV,” JHEP **1507**, 162 (2015) [arXiv:1506.06020 [hep-ex]].
- [14] G. Aad *et al.* [ATLAS Collaboration], “Search for new phenomena in the dijet mass distribution using $p - p$ collision data at $\sqrt{s} = 8$ TeV,” Phys. Rev. D **91**, no. 5, 052007 (2015) [arXiv:1407.1376 [hep-ex]].
- [15] V. Khachatryan *et al.* [CMS Collaboration], “Search for narrow resonances decaying to dijets in proton-proton collisions at $\sqrt{s} = 13$ TeV,” arXiv:1512.01224 [hep-ex].
- [16] G. Aad *et al.* [ATLAS Collaboration], “Search for new phenomena in dijet mass and angular distributions from pp collisions at $\sqrt{s} = 13$ TeV,” arXiv:1512.01530 [hep-ex].
- [17] J. Brehmer, J. Hewett, J. Kopp, T. Rizzo and J. Tattersall, “Symmetry restored in dibosons at the LHC?,” arXiv:1507.00013 [hep-ph].
- [18] A. Alloul, N. D. Christensen, C. Degrande, C. Duhr and B. Fuks, “FeynRules 2.0 - A complete toolbox for tree-level phenomenology,” Comput. Phys. Commun. **185**, 2250 (2014) [arXiv:1310.1921].
- [19] J. Alwall, R. Frederix, S. Frixione, V. Hirschi, F. Maltoni, O. Mattelaer, H.-S. Shao, T. Stelzer, P. Torrielli, M. Zaro, “The automated computation of tree-level and NLO differential cross sections, and their matching to parton shower simulations,” JHEP **1407**, 079 (2014) [arXiv:1405.0301].
- [20] Our MadGraph files are available at <http://home.fnal.gov/~bdob/WpZpDobrescuFox>
- [21] J. de Favereau *et al.* [DELPHES 3 Collaboration], “DELPHES 3, A modular framework for fast simulation of a generic collider experiment,” JHEP **1402**, 057 (2014) [arXiv:1307.6346 [hep-ex]].
- [22] R. D. Ball *et al.*, “Parton distributions with LHC data,” Nucl. Phys. B **867**, 244 (2013) [arXiv:1207.1303 [hep-ph]].

- [23] S. Heinemeyer *et al.* [LHC Higgs Cross Section Working Group Collaboration], “Handbook of LHC Higgs cross sections: 3. Higgs properties,” arXiv:1307.1347.
<https://twiki.cern.ch/twiki/bin/view/LHCPhysics/CERNYellowReportPageBR3>
- [24] D. Duffy and Z. Sullivan, “Model independent reach for W-prime bosons at the LHC,” *Phys. Rev. D* **86**, 075018 (2012) [arXiv:1208.4858 [hep-ph]].
- [25] J. M. Campbell, R. K. Ellis and W. T. Giele, “A Multi-Threaded Version of MCFM,” *Eur. Phys. J. C* **75**, no. 6, 246 (2015) [arXiv:1503.06182 [physics.comp-ph]].
- [26] Q. H. Cao, Z. Li, J. H. Yu and C. P. Yuan, “Discovery and identification of W' and Z' in $SU(2) \times SU(2) \times U(1)$ models at the LHC,” *Phys. Rev. D* **86**, 095010 (2012) [arXiv:1205.3769].
- [27] S. Chatrchyan *et al.* [CMS Collaboration], “Search for $W' \rightarrow tb$ decays in the lepton + jets final state in pp collisions at $\sqrt{s} = 8$ TeV,” *JHEP* **1405**, 108 (2014) [arXiv:1402.2176 [hep-ex]].
- [28] V. Khachatryan *et al.* [CMS Collaboration], “Search for $W' \rightarrow tb$ in proton-proton collisions at $\sqrt{s} = 8$ TeV,” arXiv:1509.06051 [hep-ex].
- [29] G. Aad *et al.* [ATLAS Collaboration], “Search for $W' \rightarrow t\bar{b}$ in the lepton plus jets final state,” *Phys. Lett. B* **743**, 235 (2015) [arXiv:1410.4103].
- [30] G. Aad *et al.* [ATLAS Collaboration], “Search for $W' \rightarrow tb \rightarrow qqbb$ decays,” *Eur. Phys. J. C* **75**, no. 4, 165 (2015) [arXiv:1408.0886];
- [31] Z. Sullivan, “Next-to-leading order $pp \rightarrow W' \rightarrow tb$ production at 14 TeV and 33 TeV,” arXiv:1308.3797 [hep-ph].
- [32] W. Y. Keung and G. Senjanovic, “Majorana neutrinos and the production of the right-handed charged gauge boson,” *Phys. Rev. Lett.* **50**, 1427 (1983).
 S. P. Das, F. F. Deppisch, O. Kittel and J. W. F. Valle, “Heavy neutrinos and lepton flavour violation in Left-Right Symmetric Models at the LHC,” *Phys. Rev. D* **86**, 055006 (2012) [arXiv:1206.0256 [hep-ph]].
 T. Han, I. Lewis, R. Ruiz and Z. g. Si, “Lepton number violation and W' chiral couplings at the LHC,” *Phys. Rev. D* **87**, no. 3, 035011 (2013) [*Phys. Rev. D* **87**, no. 3, 039906 (2013)] [arXiv:1211.6447 [hep-ph]].

- [33] F. del Aguila, J. A. Aguilar-Saavedra and J. de Blas, “Trilepton signals: the golden channel for seesaw searches at LHC,” *Acta Phys. Polon. B* **40**, 2901 (2009) [arXiv:0910.2720 [hep-ph]].
- [34] V. Khachatryan *et al.* [CMS Collaboration], “Search for massive resonances in dijet systems containing jets tagged as W or Z boson decays in pp collisions at $\sqrt{s} = 8$ TeV,” *JHEP* **1408**, 173 (2014) [arXiv:1405.1994].
- [35] The ATLAS Collaboration, “Search for WW , WZ , and ZZ resonances in pp collisions at $\sqrt{s} = 8$ TeV,” ATLAS-CONF-2015-045.
- [36] CMS Collaboration, “Search for massive resonances decaying into pairs of boosted W and Z bosons at $\sqrt{s} = 13$ TeV,” note CMS-PAS-EXO-15-002, December 2015.
- [37] ATLAS Collaboration, “Search for resonances with boson-tagged jets in 3.2 fb^{-1} of pp collisions at $\sqrt{s} = 13$ TeV,” note ATLAS-CONF-2015-073, December 2015.
- [38] ATLAS Collaboration, “Search for new resonances decaying to a W or Z boson and a Higgs boson in the $llb\bar{b}$, $l\nu b\bar{b}$, and $\nu\nu b\bar{b}$ channels in pp collisions at $\sqrt{s} = 13$ TeV,” note ATLAS-CONF-2015-074, December 2015.
- [39] S. P. Liew and S. Shirai, “Testing ATLAS diboson excess with dark matter searches at LHC,” arXiv:1507.08273 [hep-ph].
- [40] CMS Collaboration, “Search for New Physics in the V-jet + MET final state,” CMS-PAS-EXO-12-055.
- [41] V. Khachatryan *et al.* [CMS Collaboration], “Search for dark matter, extra dimensions, and unparticles in monojet events in proton-proton collisions at $\sqrt{s} = 8$ TeV,” *Eur. Phys. J. C* **75**, no. 5, 235 (2015) [arXiv:1408.3583 [hep-ex]].
- [42] G. Aad *et al.* [ATLAS Collaboration], “Search for new phenomena in final states with an energetic jet and large missing transverse momentum in pp collisions at $\sqrt{s} = 8$ TeV,” *Eur. Phys. J. C* **75**, no. 7, 299 (2015) [*Eur. Phys. J. C* **75**, no. 9, 408 (2015)] [arXiv:1502.01518 [hep-ex]].
- [43] B. A. Dobrescu and A. D. Peterson, “ W' signatures with odd Higgs particles,” *JHEP* **1408**, 078 (2014) [arXiv:1312.1999].
A. Jinaru, C. Alexa, I. Caprini and A. Tudorache, “ $W' \rightarrow hH^\pm$ decay in $G(221)$ models,” *J. Phys. G* **41**, 075001 (2014) [arXiv:1312.4268].

- [44] J. Hisano, N. Nagata and Y. Omura, “Interpretations of the ATLAS Diboson Resonances,” *Phys. Rev. D* **92**, no. 5, 055001 (2015) [arXiv:1506.03931 [hep-ph]].
- [45] J. H. Collins and W. H. Ng, “A 2 TeV W_R , Supersymmetry, and the Higgs Mass,” arXiv:1510.08083 [hep-ph].
Q. H. Cao, B. Yan and D. M. Zhang, “Simple Non-Abelian Extensions and Diboson Excesses at the LHC,” arXiv:1507.00268 [hep-ph].
- [46] G. Aad *et al.* [ATLAS Collaboration], “Search for high-mass dilepton resonances in pp collisions at $\sqrt{s} = 8$ TeV,” *Phys. Rev. D* **90**, no. 5, 052005 (2014) [arXiv:1405.4123].
- [47] V. Khachatryan *et al.* [CMS Collaboration], “Search for physics beyond the standard model in dilepton mass spectra in proton-proton collisions at $\sqrt{s} = 8$ TeV,” *JHEP* **1504**, 025 (2015) [arXiv:1412.6302 [hep-ex]].
- [48] CMS Collaboration, “Event display of a candidate electron-positron pair with an invariant mass of 2.9 TeV”, note CMS-DP-2015-039, Aug. 2015.
- [49] CMS Collaboration, “Search for a narrow resonance produced in 13 TeV pp collisions decaying to electron pair or muon pair final states,” note CMS-PAS-EXO-15-005, December 2015.
- [50] ATLAS Collaboration, “Search for new phenomena in the dilepton final state using proton-proton collisions at $\sqrt{s} = 13$ TeV,” note ATLAS-CONF-2015-070, December 2015.